3GPP TSG RAN WG1 Meeting #55 **R1-084491**
Prague, Czech Republic, 10th to 14nd November 2008

Agenda Item:	11.3
Source:	STMicroelectronics
Title:	Feedback and Precoding Techniques for MU-MIMO for LTE-A
Document for:	Discussion

1. Introduction

MU-MIMO is of particular interest for LTE-A because of its ability to increase total cell throughput rather than simply providing very high peak data rates to a small proportion of the UEs in the cell. In this paper we motivate the need of possible enhancements to MU-MIMO which have the potential to increase system capacity compared to LTE Rel-8.
The capacity of the generic MU-MIMO downlink is known to be heavily dependent on the quality of channel state information at the transmitter (CSIT) [1]. Optimal precoding strategies based on the dirty-paper coding theorem [2] are still too complex to be implemented in practical systems. However, suboptimal linear techniques such as zero-forcing beamforming (ZFBF) or regularized ZFBF (R-ZFBF) achieve the full multiplexing gain when perfect CSIT is available [3]. In practice, CSIT can usually be obtained via feedback from the UE to the eNodeB. Thus, the quality of the CSIT is impacted by the a number of aspects of the feedback: the measurement error, any quantisation granularity, the data rate of the feedback signalling, transmission errors in the feedback signalling and the delay of the feedback signalling. For simplicity for the initial evaluations presented here we consider the case of no measurement error, and error-free zero-delay transmission of the (quantised) feedback signalling. Hence, the quality of the CSIT is solely determined by the feedback rate (results which take into account all sources of errors will be presented in the future). It has been shown in [4] that, in order to achieve the full multiplexing gain, the necessary number of feedback bits B for ZFBF and R-ZFBF scales *linearly* with the signal-to-noise ratio (SNR [dB]). If B is fixed then the throughput is interference-limited. For example: Consider a 4×4 MIMO system operating at a SNR of 25 dB. To maintain a 3 dB SNR gap between ZFBF with perfect CSIT and ZFBF with limited feedback, 25 feedback bits per UE are required.
In this contribution we show the potential benefits of improving the quality of the channel state feedback for a given number of feedback bits. We compare the achievable sum rate for ZFBF and R-ZFBF algorithms and unitary beamforming (UBF) strategies in case of perfect CSIT and we analyze the sensitivity of these beamforming algorithms to the error in the feedback. We also compare the performance as a function of the channel orthogonality of the UEs (with perfect CSIT). This makes it possible to see the gap between the different schemes when the UE channel orthogonality is not close to optimal.

2. System Model

We consider a MU-MIMO system where the eNodeB is equipped with M transmit antennas and serves K single-antenna UEs. The received signal of UE i is

$$y_i = \sum_{j=1}^{K} \mathbf{h}_i^{\mathsf{H}} \mathbf{v}_j s_j + n_i \quad (1)$$

where $\mathbf{h}_i \in \mathbb{C}^{M\times 1}$ $(i = 1, 2, \ldots, K)$ describes the channel from the eNodeB to UE i. All K channels can be assembled in $\mathbf{H}^{\mathsf{H}} = [\mathbf{h}_1 \mathbf{h}_2 \ldots \mathbf{h}_K]\,, \mathbf{H} \in \mathbb{C}^{K\times M}$. Each symbol s_j is multiplied by the beamforming vector $\mathbf{v}_j$ to form the transmit signal $\mathbf{x} = \sum_{j=1}^{K} \mathbf{v}_j s_j$. We assume equal power allocation i.e. $\|s_j\|^2 = \frac{P}{M}$. The additive noise $\{n_i\}$ are assumed to be independent and complex Gaussian distributed with zero mean and variance σ_n^2.
The received signal-to-interference plus noise ratio (SINR) of each UE for for linear precoding is given by

$$\gamma_i = \frac{|\mathbf{h}_i^{\mathsf{H}} \mathbf{v}_i|^2}{\sum_{j\neq i} |\mathbf{h}_i^{\mathsf{H}} \mathbf{v}_j|^2 + \frac{M\sigma_{\mathrm{n}}^2}{P}} \quad (2)$$

If the symbols s_j are i.i.d. complex Gaussian the *long-term* achievable sum rate is

$$\mathcal{R} = M \mathrm{E}_{\mathbf{H}} \left[\log_2(1 + \gamma_i)\right] \quad \text{bit/s/Hz} \quad (3)$$

3. Linear Precoding Techniques

This section briefly reviews the linear precoding techniques that are compared in this contribution. The linear precoding scheme which maximizes the sum rate (3) can be found in [5].

The ZFBF vectors are obtained by simply inverting the channel vectors $\mathbf{h}_i$ [3] i.e. if $K < M$

$$\mathbf{V}_{zf} = \frac{1}{\lambda} \mathbf{H}^{\mathsf{H}} \left(\mathbf{H}\mathbf{H}^{\mathsf{H}}\right)^{-1} \quad (4)$$

where $\frac{1}{\lambda} = \sqrt{\frac{1}{P} \mathrm{tr}\left((\mathbf{H}\mathbf{H}^{\mathsf{H}})^{-1}\right)}$ is the scaling factor to fulfill the sum-power constraint. If $K = M$ we have $\mathbf{V}_{zf} = \mathbf{H}^{-1}$. In case of R-ZFBF we have

$$\mathbf{V}_{rzf} = \frac{1}{\lambda} \mathbf{H}^{\mathsf{H}} \left(\mathbf{H}\mathbf{H}^{\mathsf{H}} + \alpha \mathbf{I}\right)^{-1} \quad (5)$$

where $\frac{1}{\lambda}$ is chosen such that $\mathrm{tr}(\mathbf{V}_{rzf} \mathbf{V}_{rzf}^{\mathsf{H}}) = P$ and $\alpha = K/\mathsf{SNR}$ (large-K approximation), [3].

In practice, a common assumption is that the power amplifiers (PA) for the different transmit antennas at the eNodeB are balanced on average i.e. $\mathrm{E}[\mathbf{x}\mathbf{x}]^{\mathsf{H}} = \frac{P}{M}\mathbf{I}$. On average all linear precoder meet this constraint as the channel becomes i.i.d. Gaussian. Unitary BF has the

advantage that the SINR at the UEs can be computed exactly as the beamforming vectors are mutually orthogonal. Unfortunately there is no closed-form expression of the BF vectors for unitary beamforming (UBF). To compute the optimal UBF, an iterative algorithm based on successive Givens rotations has been proposed in [6]. In this contribution we apply this iterative algorithm to evaluate the performance of the UBF.
A performance comparison of various UBF schemes can be found in [7].

4. Simulation And Results

In this section we compare different precoding and feedback schemes in terms of *ergodic* sum rate (3) which indicates the performance averaged over all channel realizations. We assume $M = K$ and, for these initial results, we do not implement a user scheduling technique.

4.1. Perfect CSIT

As the sum rate of the MU-MIMO downlink channel is highly dependent on the quality of the CSIT we first compare ZFBF, R-ZFBF and UBF when perfect CSI is available at the eNodeB. The DPC performance is plotted along and gives the upper bound on the achievable sum rate. From Figure 1 we observe that ZFBF and R-ZFBF achieve the full multiplexing gain of M i.e. the curves have a slope of M bit/s/Hz/3 dB at high SNR. As expected the curves of ZFBF and R-ZFBF merge as the SNR increases. The rate-gap from the optimal dirty-paper coding (DPC) algorithm is approximately $3 \log_2 M$ dB i.e. ≈ 6 dB, [8].
UBF outperforms ZFBF for low SNR but becomes interference-limited in the medium and high SNR region. **As a conclusion we clearly observe that ZFBF and R-ZFBF achieve significant sum rate gains with respect to UBF for high SNR.**

A possible user scheduling strategy may only select UEs that are close to orthogonal. Thus, there is a need to evaluate the performance of the various precoding schemes for near-orthogonal channels. As a measure of orthogonality we utilize the *orthogonal deficiency*

$$\mathrm{od}(\mathbf{H}) = 1 - \frac{\det(\mathbf{H}\mathbf{H}^{\mathsf{H}})}{\prod_{i=1}^{K} \|\mathbf{h}_i^{\mathsf{H}}\mathbf{h}_i\|^2} \text{ with } \mathrm{od}(\mathbf{H}) = \begin{cases} 1 & \to \mathbf{H} \text{ is singular} \\ 0 & \to \mathbf{H} \text{ fully orthogonal} \end{cases} \tag{6}$$

Figure 2 shows the performance of DPC, (R)-ZFBF and UBF for near-orthogonal channels. Note that all three schemes achieve the same performance if the channel is fully orthogonal (this point is not shown in the figure). The performance of ZFBF decreases rapidly if the channel matrix becomes close to singular
As a conclusion we clearly observe that ZFBF is more sensitive than UBF and R-ZFBF to the loss of orthogonality and care should be taken in selecting users.

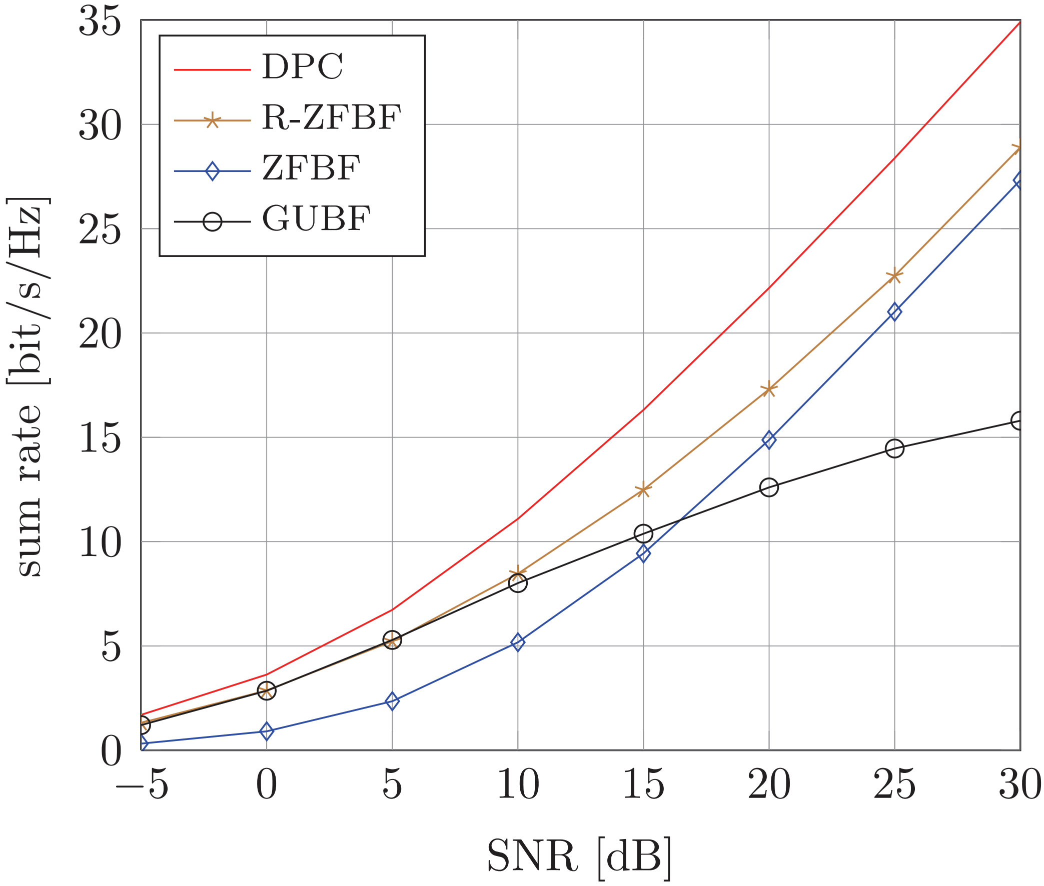

Figure 1: 4×4 MIMO independent Rayleigh fading channel, 1e3 channel realizations

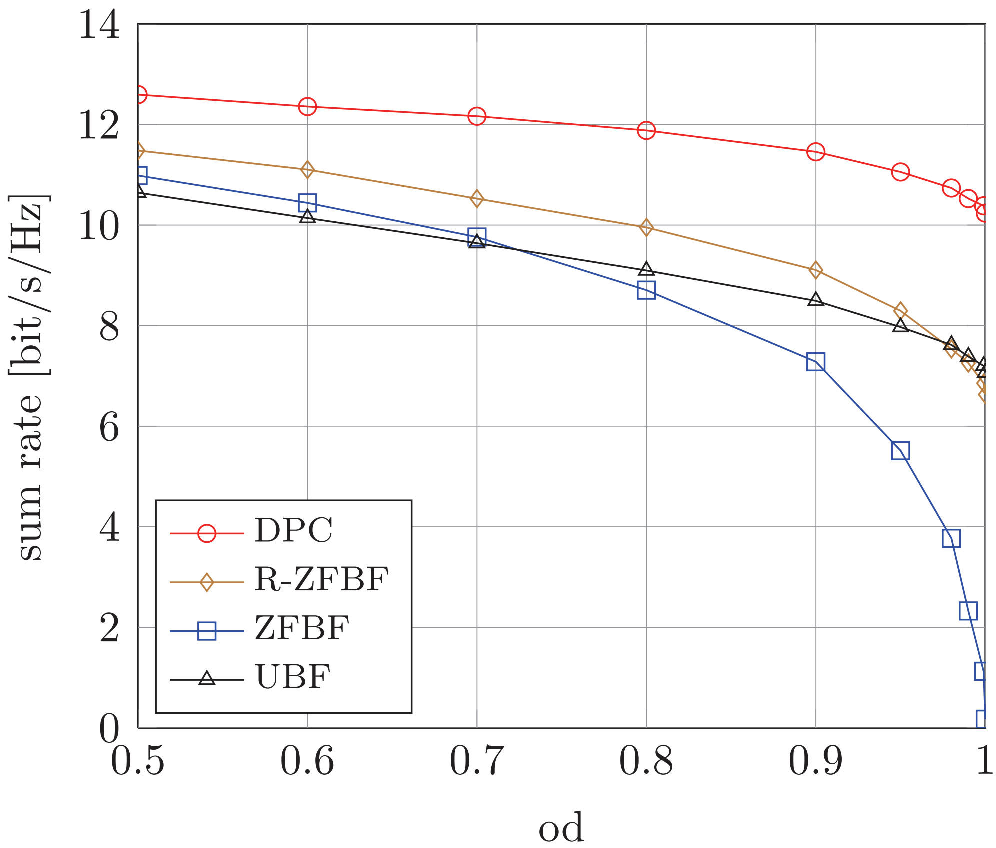

Figure 2: 4×4 MIMO independent Rayleigh fading channel, SNR = 10 dB

4.2. Sensitivity to erroneous CSIT

As shown in the previous subsection perfect CSIT allows for high sum rates. Now we analyze the impact of noisy CSIT on the performance of the various precoding techniques, by assuming that the errors in the CSIT are i.i.d and Gaussian distributed. The imperfect CSIT is modeled as

$$\hat{\mathbf{H}} = \sqrt{1-\sigma^2}\mathbf{H} + \sigma\mathbf{N} \tag{7}$$

where the matrices $\mathbf{H}$ and $\mathbf{N}$ have standard Gaussian i.i.d. entries. A more extensive study of CSIT imperfection with respect to channel estimation can be found in [9].

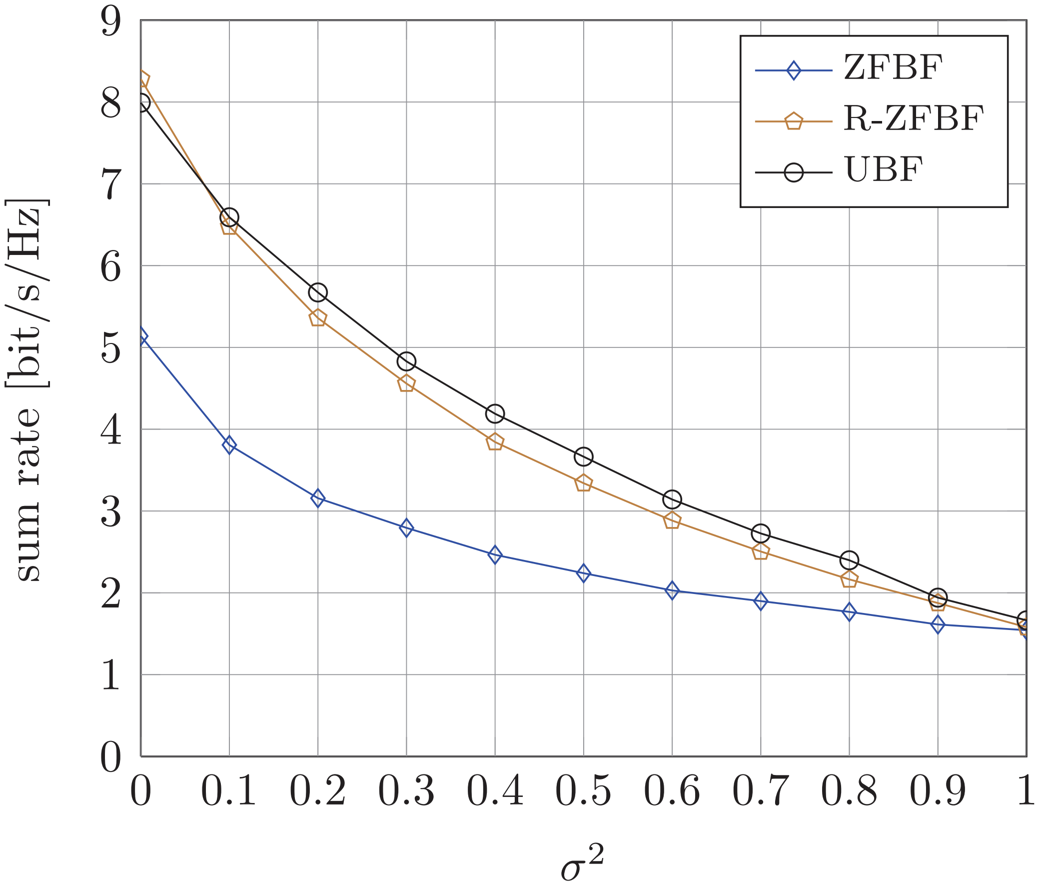

Figure 3: Independent Rayleigh-fading channel, 1000 channel realizations, 4×4 MIMO, SNR $= 10$ dB.

In Figure 3 we observe that the UBF slightly outperforms R-ZFBF for low-quality CSIT i.e. if σ^2 exceeds approximately 0.08. Furthermore we see that R-ZFBF, ZFBF and UBF have the same slope and hence the same sensitivity to errors in the CSIT. Figure 4 compares the distortion achieved when a constant channel is quantized with a Random Vector Quantizer (RVQ)[1]

[1] Note that the channel is constant i.e. RVQ is only applied once for the first CSI report

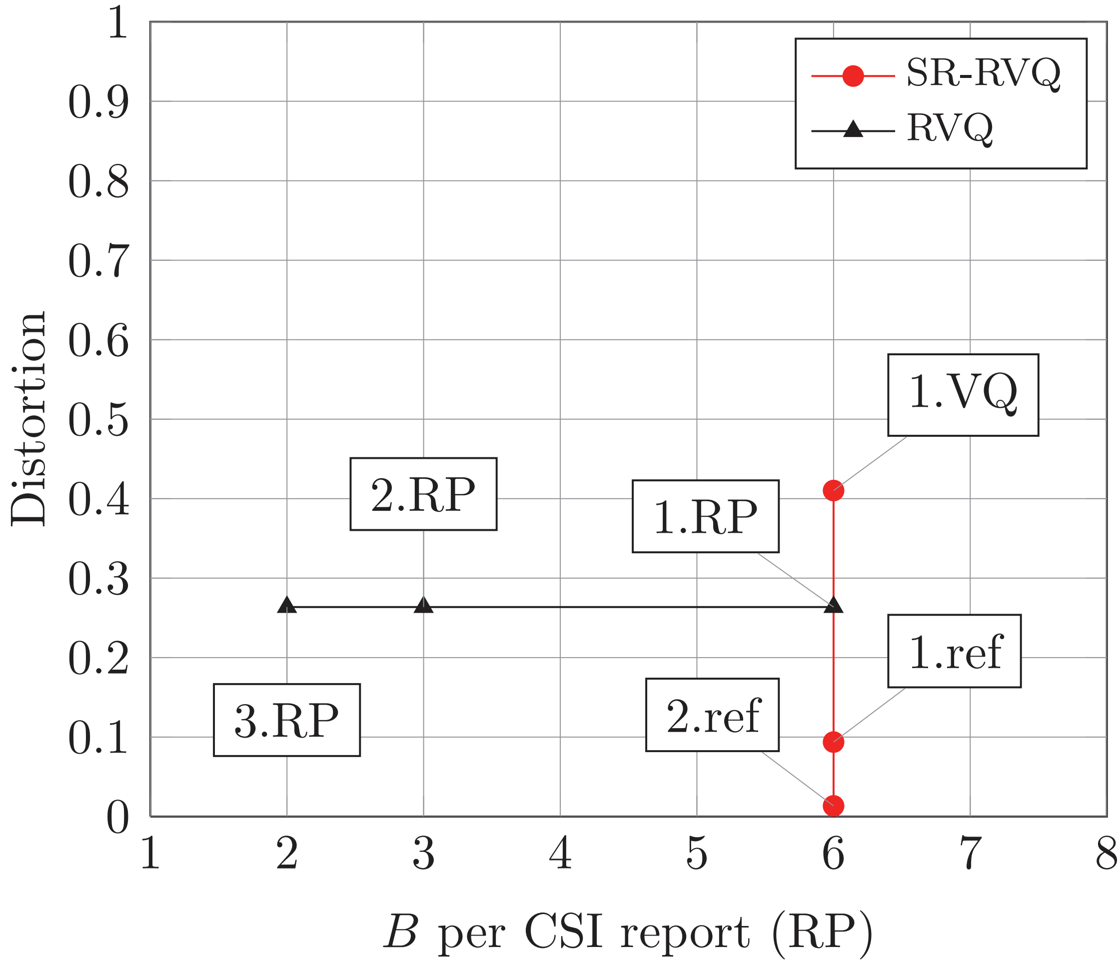

Figure 4: Independent Rayleigh-fading channel, 1000 channel realizations, $M = 4$, $K = 1$.

with a successive refinement (SR) scheme as described in [10]. To assure a fair comparison we also use RVQ in the SR scheme at each refinement step.
The shared RVQ codebook $\mathcal{W} = \{\mathbf{w}_1, \dots, \mathbf{w}_{2^B}\}$ of size 2^B is generated as in [4] and references therein. Here, the quantisation vectors are isotropically distributed on the M-dimensional unit sphere and the UE computes the codeword index L_i according to the chordal distance

$$L_i = \arg \min_{j=1,\dots,2^B} \sin^2\left(\angle(\mathbf{h}_i, \mathbf{w}_j)\right) \tag{8}$$

Figure 4 shows that the RVQ with 6 bit leads to a distortion [2] of about 0.3.

Under the successive refinement [10], the reported CSI is made more accurate with each successive CSI report. The first step is equivalent to a classical vector quantisation. At *each* subsequent step, a refinement is performed, consisting of the following operations:

1. Compute the error vector between the selected quantized vector and the actual measured channel vector (chordal distance)
2. Rotate the $M - n$ dimension codebook into the $M - n$ space orthogonal to the reconstruction vector at step $n - 1$, where n is the index of the refinement step
3. Do a vector quantisation and signal (by using $\log_2(M)$ bits) the corresponding refinement step

Appendix A.1 shows a pictorial representation of the successive refinement scheme for $M = 3$ real dimensions.
Figure 4 shows that the distortion after two refinement steps has been reduced to about 0.01. This distortion reduction leads to a gain of 2 bit/s/Hz for ZFBF (see Figure 3).
As a conclusion we see that reducing the distortion of the feedback leads to a significant performance gain.

4.3. Precoding with Limited Feedback

In this section we compare different limited feedback precoding strategies. We assume $B = 6$ bit for each feedback codeword. Thus, for the SR scheme we either use a Grassmannian codebook of size $B = 4$ (SR-GM) or a RVQ (SR-RVQ) at each of the 3 quantisation steps. The remaining two bit are used to signal the current refinement step. The RVQ [3] is carried out with $B = 6$. Furthermore the channel is constant over a block so that the channel vectors are maximally refined.
Figures 5, 6 and 7 reveal a significant sum rate gain for (R-)ZFBF and UBF respectively, if the CSIT is successively refined and not just directly quantised as in RVQ. The rate-gap between SR and RVQ at a SNR of 20 dB is about 14 bit/s/Hz for ZFBF and approximately 8 bit/s/Hz in case of UBF.

[2] As a distortion measure we use the euclidean distance i.e. $d = \|\mathbf{h} - \hat{\mathbf{h}}\|^2$
[3] In this contribution the RVQ is constructed following [4]

When the channel is time-varying, the same successive refinement algorithm can be applied. But the probability that two consecutive channel vectors will be quantised with same codeword decreases if the channel is changing fast in time. In the worst case, when there is no correlation between two consecutive instances of the channel, the SR approach reduces to a RVQ at each step. However, in general we expect such MU-MIMO techniques to be most likely applied in low-mobility scenarios where the time correlation of the channel can be exploited to increase the cell throughput.

Simulation results for time varying channels will be provided in future contributions.

As an initial conclusion, we observe that for high SNR, ZFBF outperforms UBF if high-quality CSI is available at the eNodeB. At least in static/slow time varying channels, feedback schemes such as SR allow a close-to-optimal performance of linear precoding techniques.

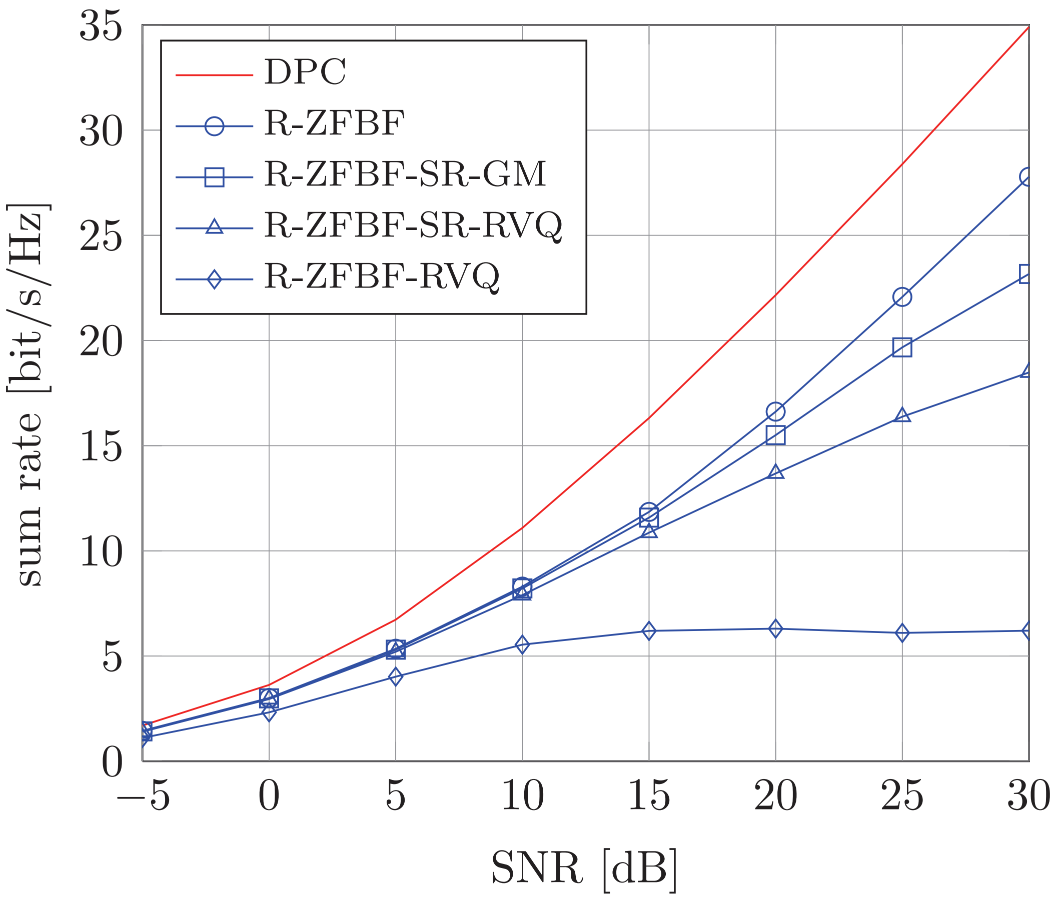

Figure 5: 4×4 MIMO independent Rayleigh-fading channel, 1e4 channel realizations, regularized zero-forcing BF (R-ZFBF)

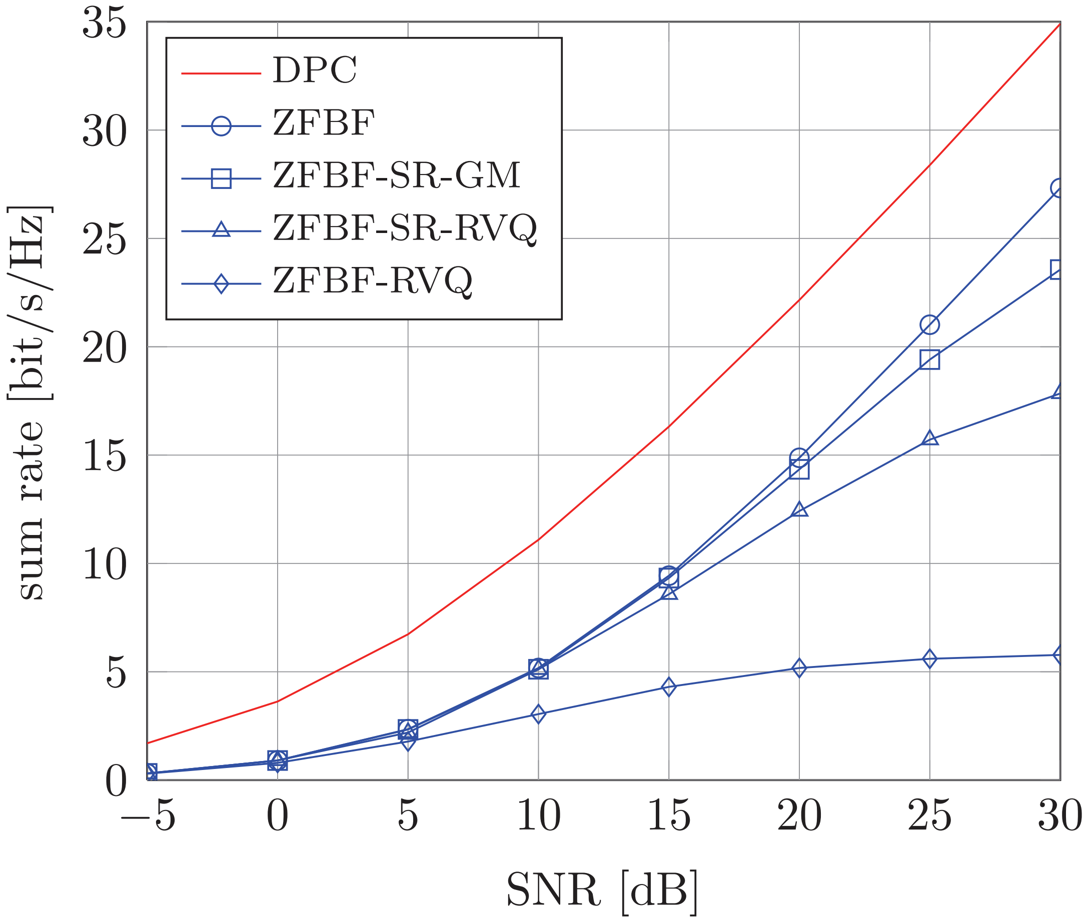

Figure 6: 4×4 MIMO independent Rayleigh-fading channel, 1e4 channel realizations, zero-forcing BF (ZFBF)

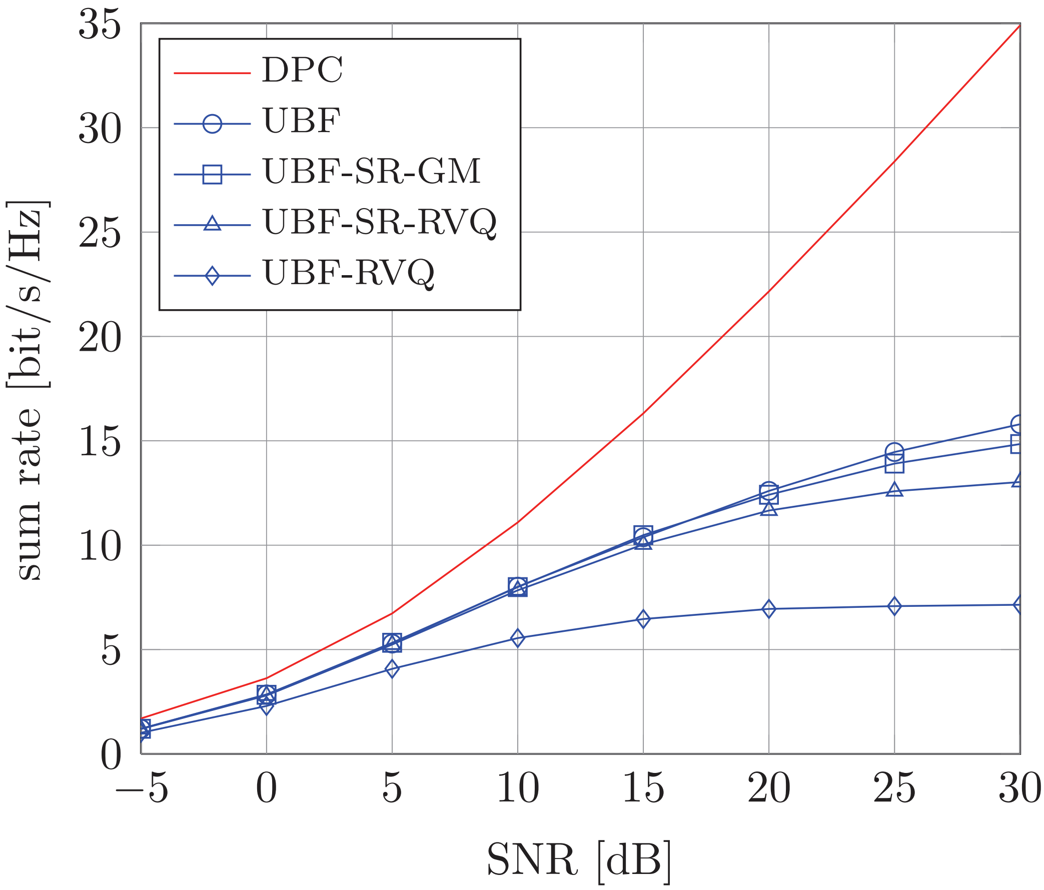

Figure 7: 4×4 MIMO independent Rayleigh-fading channel, 1e4 channel realizations, unitary BF (UBF)

5. Conclusions

From this initial study of several possible MU-MIMO extensions aiming to enhance the system throughput in LTE-A, we conclude the following:

1. R-ZFBF shows the best results when perfect CSIT is available. UBF outperforms ZFBF for low/medium SNR.
2. Reducing the error of the channel state feedback increases the total cell throughput.
3. Successive refinement of channel state feedback has the potential to reduce the feedback error and thus to significantly increase system throughput, at least in low-mobility scenarios.

A. Appendix

A.1. Details On Successive Refinement Algorithm

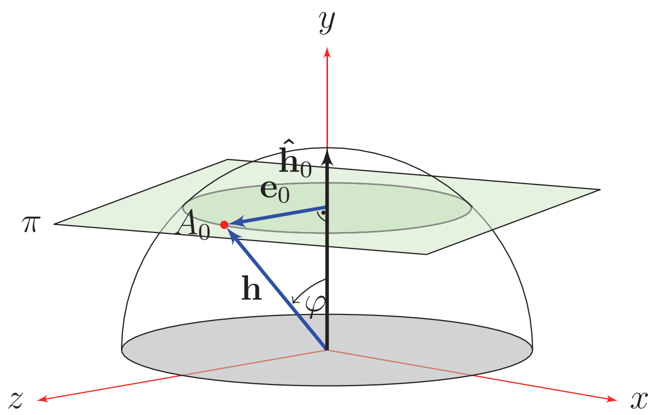

Figure 8: Refinement Step 0

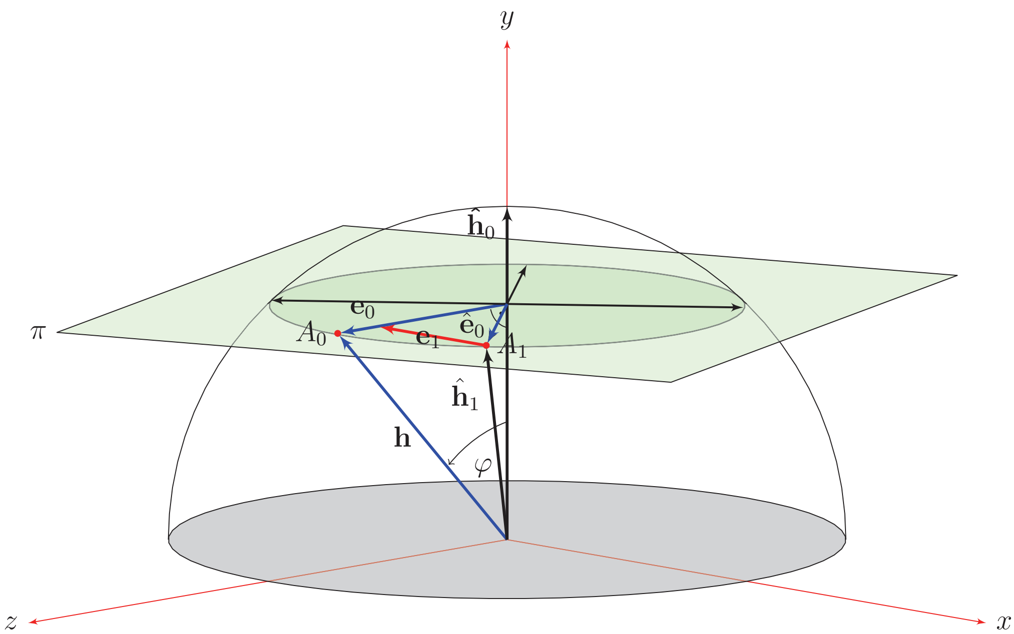

Figure 9: Refinement Step 1

References

[1] G. Caire and S. Shamai (Shitz), "On the achievable throughput of a multiantenna Gaussian broadcast channel", *IEEE Trans. on Information Theory*, Vol. 49, No. 7, pp. 1691-1706, July 2003

[2] M. H. M. Costa, "Writing on Dirty Paper", *IEEE Trans. on Information Theory*, Vol. IT-29, No. 3, May 1983

[3] C. B. Peel, B. M. Hochwald and A. L. Swindlehurst, "A Vector-Perturbation Technique for Near-Capacity Multiantenna Multiuser Communication–Part I: Channel Inversion and Regularization" *IEEE Trans. on Communications*, Vol. 53, No. 1, pp. 195-202, January 2005

[4] N. Jindal, "MIMO Broadcast Channels With Finite-Rate Feedback" *IEEE Trans. on Information Theory*, Vol. 52, No. 11, pp. 5045-5060, November 2006

[5] M. Stojnic, H. Vikalo and B. Hassibi, "Rate Maximization in Multi-Antenna Broadcast Channels with Linear Preprocessing" *IEEE Trans. on Wireless Communications*, Vol. 5, No. 9, September 2006

[6] R. de Francisco and D. T. M. Slock, "An iterative Optimization Method for Unitary Beamforming in MIMO Broadcast Channels", *Proc. of 45th Allerton Conf. on Commun., Control and Comput.*, pp. 360-367, September 2007

[7] STMicroelectronics, “Unitary beamforming for MU-MIMO with per-antenna power contraint for LTE-A”, 3GPP TSG RAN WG1 Meeting #55, November, 2008

[8] N. Jindal, “High SNR Analysis of MIMO Broadcast Channels”, *Proc. IEEE Int. Symp. Information Theory*, pp. 2310-2314, September 2005

[9] STMicroelectronics, “Reliability of the channel knowledge at the eNodeB for MU-MIMO systems”, 3GPP TSG RAN WG1 Meeting #55, November, 2008.

[10] Philips, NXP Semiconductors, “Vector quantisation with successive refinement for MIMO feedback”, 3GPP TSG RAN WG1 Meeting #49bis, June, 2007